



HAL
open science

Phosphine-based push-pull AIE fluorophores: Synthesis, photophysical properties, and TD-DFT studies

Maxime Rémond, Pauline Colinet, Erwan Jeanneau, Tangui Le Bahers, Chantal Andraud, Yann Bretonnière

► To cite this version:

Maxime Rémond, Pauline Colinet, Erwan Jeanneau, Tangui Le Bahers, Chantal Andraud, et al.. Phosphine-based push-pull AIE fluorophores: Synthesis, photophysical properties, and TD-DFT studies. *Dyes and Pigments*, 2021, 193 (1), pp.109485. 10.1016/j.dyepig.2021.109485 . hal-03821202

HAL Id: hal-03821202

<https://hal.science/hal-03821202v1>

Submitted on 13 Jun 2023

HAL is a multi-disciplinary open access archive for the deposit and dissemination of scientific research documents, whether they are published or not. The documents may come from teaching and research institutions in France or abroad, or from public or private research centers.

L'archive ouverte pluridisciplinaire **HAL**, est destinée au dépôt et à la diffusion de documents scientifiques de niveau recherche, publiés ou non, émanant des établissements d'enseignement et de recherche français ou étrangers, des laboratoires publics ou privés.



Distributed under a Creative Commons Attribution - NonCommercial 4.0 International License

1 Phosphine-based Push-Pull AIE Fluorophores: Synthesis, 2 Photophysical Properties, and TD-DFT Studies.

3 Maxime Rémond,^a Pauline Colinet,^a Erwan Jeanneau,^b Tangui Le Bahers,^a
4 Chantal Andraud,^a Yann Bretonnière^a

5 ^a *Université de Lyon, École Normale Supérieure de Lyon, Université Lyon 1, CNRS UMR*
6 *5182, Laboratoire de Chimie, 46 allée d'Italie, 69364 Lyon (France)*

7 ^b *Université de Lyon, Centre de Diffractométrie Henri Longchambon, Université Lyon 1, 43*
8 *boulevard du 11 Novembre 1918, 69622 Villeurbanne Cedex (France)*

9 Abstract

10 Herein, we report the design and characterization of a novel series of four push-pull
11 fluorophores using diphenylphosphino as an electron-donating terminal group (P-
12 chromophores). The spectroscopic properties in solution, the aggregation-induced emission
13 (AIE) properties, as well as the emission properties in the solid state were studied and
14 compared with those of the diphenylamino-analogues (N-chromophores). Comparative
15 analysis of the crystalline structures coupled with density functional theory calculations
16 revealed that the diphenylphosphino group adopts a pyramidal geometry, whereas a trigonal
17 planar configuration around the N-center is observed for the diphenylamino group.
18 Consequently, the phosphorous lone pair is localized on the upper side of the average
19 chromophore plan and considerable geometrical change of the P-center can occur between
20 the ground state and the first excited state, explaining the much larger Stokes shift observed
21 (10,000 cm⁻¹) for the P-chromophores compared to the N-analogues.

22 Keywords

23 Phosphine based dyes – Push-pull dyes – DFT – AIE – Large Stokes shift

24 1 Introduction

25 Organic synthesis offers virtually endless possibilities to fine-tune the optical properties of
26 organic fluorophores. To this end, the incorporation of heteroatoms into the chromophore π -
27 backbone is an effective structure-modification strategy inducing significant electronic

1 perturbations in the parent molecules and, usually, a large wavelength shift. While light main-
2 group heteroatoms such as boron (B), nitrogen (N), or oxygen (O) have been extensively
3 used,[1-3] heavier second-row elements such as phosphorous (P) have been rather neglected,
4 especially in small push-pull molecules. However, straightforward chemical transformations
5 of the P-center through oxidation/reduction, complexation with metal ion or quaternarization
6 provides numerous options to modulate the photophysical and electrochemical properties of
7 π -electron frameworks in which the P-center is embedded or grafted. $\lambda^5\sigma^4$ (phosphorus oxide
8 or sulfide) and $\lambda^4\sigma^4$ phosphorus groups (phosphonium cations) behave as strong electron-
9 withdrawing groups [4-6] but has only seldom been used as such in simple combination with
10 donor groups to construct dipolar rod-shaped [7-12] or three-dimensional star-shaped
11 octupolar chromophores.[10, 12, 13]

12 By contrast, $\lambda^5\sigma^4$ and $\lambda^4\sigma^4$ P-heterocyclic compounds, containing either a five-membered
13 phosphole ring [14-23] or six-membered ring variants,[24-37] showed great potential for the
14 construction of interesting far-red emissive π -conjugated structures. The obtained cyclic-
15 organophosphorous derivatives differ from their widely used sulphur or nitrogen analogues
16 by a substantial bathochromic shift of absorption and emission up to the NIR.[25, 30, 34]
17 This can be ascribed to the lower aromaticity bestowed by specific orbital interactions
18 between the exocyclic $\sigma^*(\text{P-R})$ or $\sigma^*(\text{P=O})$ and π^* (butadiene) orbitals, together with the
19 pyramidal configuration of the phosphorus atom.[14, 17, 18]

20 Besides phosphole derivatives, there are few examples of chromophores containing a $\lambda^3\sigma^3$ P-
21 center in general and phosphine particularly. The lesser interest for P(III) can be explained by
22 its sensitivity towards oxidation, particularly in solution, which limits synthetic yields,
23 spectroscopic studies and final applications. However, P(III) to P(V) oxidation can be
24 prevented by delocalization of the lone pair in a π -system. Thus, conjugated phosphines, such
25 as triphenylphosphine or BINAP, are quite stable towards oxidation. Using this strategy,
26 stable primary or tertiary phosphines linked to a BODIPY derivative were synthesized by
27 Higham *et al.* for metal sensing.[38, 39] However, this approach can be limited by potential
28 fluorophore quenching due to a photoinduced electron transfer to the nearby phosphine.[40,
29 41] Fluorescent $\lambda^3\sigma^3$ phosphines were nevertheless obtained by either including the
30 phosphorus atom in a fused π system [42] or with three extended π -systems around the
31 phosphorus atom.[43] It is also possible to use the electron donating capacities of phosphines
32 to design intramolecular charge transfer dyes. For example, Madrigal *et al.* studied the
33 absorption properties of quadripolar and octupolar triphenylamine and triphenylphosphine

1 stilbene derivatives.[44-46] The absorption and non-linear optical properties of a dipolar dye
2 containing a phosphine donor and a nitro acceptor, as well as a few donor/acceptor structures,
3 based on an aryl phosphine coupled with a boron acceptor, were also investigated.[47, 48]
4 Finally, Baumgartner *et al.* studied 2,7-diketophosphepin as fluorescent π -conjugated
5 building blocks.[49] Interestingly, some of those compounds showed solid-state emission, but
6 quantum yields were not reported.

7 Hence, only a few examples of fluorescent phosphine derivatives have been studied, even
8 fewer in a push-pull configuration, and none of them emit in the biological window (650 nm -
9 1000 nm) for imaging applications. It appears that more studies of these derivatives are called
10 for. Indeed, thanks to the intramolecular charge transfer from the donor to the acceptor end,
11 these chromophores have unique optical properties such as a large Stoke shift that any
12 variation of the donor or the acceptor end will modify.

13 Herein, we used P- $\lambda^3\sigma^3$ triphenylphosphine as the donor group in a series of small push-pull
14 fluorophores (**P1-P4**, Figure 1) incorporating various potent electron acceptor groups **1-4**.
15 The optical properties in solution but also in the solid state were measured and compared
16 with those of the triphenylamine analogues (**N1-N4**) that we reported previously.[50-52] The
17 influence of the donor atom on the optical properties was rationalized by comparison with the
18 X-ray diffraction structures and by theoretical calculations. In particular, we showed that
19 conformational changes around the P-atom between the ground state and the first excited
20 state led to higher fluorescence turn-on coefficients upon aggregation (170-fold increase
21 emission for **P2**) than their amine analogues, as well as a drastically increased Stokes shift
22 (up to 10 000 cm^{-1} on average).

23 **2 Materials and methods**

24 **2.1 General**

25 Commercially available materials were used as received. Analytical thin-layer
26 chromatography (TLC) was carried out on Merck 60 F254 precoated silica gel plate (0.2 mm
27 thickness). Visualization was performed using a UV lamp (254 nm or 365 nm). Anhydrous
28 THF was distilled over sodium and benzophenone. Microwave synthesis were conducted in
29 10 mL sealed tube on a Biotage Initiator 2.5 single-mode reactor using external IR
30 temperature control. Column chromatography was performed on Merck silica gel Si-60 (40-
31 63 μm). NMR spectra were recorded at ambient temperature on a standard spectrometer

1 operating at 400 MHz or 300 MHz for ^1H NMR, 125 MHz or 101 MHz for ^{13}C NMR and
2 202 MHz or 162 MHz for ^{31}P NMR. Chemical shifts are given in parts per million (ppm,) and
3 are reported relative to tetramethylsilane (^1H , ^{13}C) using the residual solvent peaks as internal
4 standard. ^1H NMR splitting patterns are designated as singlet (s), doublet (d), triplet (t),
5 quartet (q), dd (doublet of doublets), q (quadruplet), quint (quintuplet) or m (multiplet). Low
6 resolution mass spectra were measured at 298 K by direct injection of dilute sample into the
7 mass analyzer of an Agilent Technologies 1260 Infinity LC-MS instrument. High-resolution
8 mass spectrometry (HRMS) measurements were performed by ESI-QTOF mass spectrometry
9 (Bruker Daltonics MicroTOF-Q II) at the *Centre Commun de Spectrométrie de Masse*
10 (UCBL, Villeurbanne, France). Compound **1**,^[53] **2** and **3**,^[52] and **4** ^[50] were obtained
11 according to reported procedure.

12 **2.2 Synthetic procedures and characterization data**

13 **2.2.1 2-(4-Bromophenyl)-1,3-dioxolane.**^[54-56] 4-Bromobenzaldehyde (2 g, 10.8
14 mmol) and p-toluenesulfonic acid (0.2 g, 1 mmol) were dissolved in toluene (50 mL), and an
15 excess of ethylene glycol (2 mL, 35 mmol) was added. The mixture was then heated to reflux
16 overnight with azeotropic removal of water by a Dean–Stark trap. After cooling, the solution
17 was washed three times with saturated aqueous Na_2CO_3 , dried over Na_2SO_4 , filtrated and
18 concentrated. Purification by column chromatography on silica eluting with
19 CH_2Cl_2 /petroleum ether (v/v 1:1) gave a white solid (2.3 g, 93 %). ^1H -NMR (300 MHz,
20 CDCl_3 , δ /ppm) 7.51 (d, $J = 8.4$ Hz, 2H), 7.35 (d, $J = 8.4$ Hz, 2H), 5.77 (s, 1H), 4.15–3.98 (m,
21 4H); $^{13}\text{C}\{^1\text{H}\}$ -NMR (100 MHz, CDCl_3 , δ /ppm) 137.2, 131.7, 128.3, 123.4, 103.2, 65.5; HR-
22 MS (ESI-QTOF, pos) m/z calcd for $\text{C}_9\text{H}_9\text{BrO}_2$: 227.9780 $[\text{M}]^+$, found: 227.9751.

23 **2.2.2 2-(Diphenylphosphino)-1,3-dioxolane.**^[57-59] 2-(4-Bromophenyl)-1,3-dioxolane
24 (2.2 g, 9.6 mmol) was dissolved in anhydrous THF under argon and cooled to -78 °C. *n*BuLi
25 (2.5 M in hexanes, 4.25 mL, 10.6 mmol) was added dropwise and the mixture was stirred for
26 1 hour at -78 °C. Chlorodiphenylphosphine (2.2 g, 10 mmol) in anhydrous THF (5 mL) was
27 then added dropwise. The temperature was let heat up to RT and the solution was stirred
28 overnight. The reaction was quenched with saturated NH_4Cl (4 mL) and the layers were
29 separated. The organic layer was washed with water and brine, dried over Na_2SO_4 , filtered
30 and concentrated under vacuum to give a yellow oil. The product was purified over silica gel
31 chromatography eluting with CH_2Cl_2 and a white solid was obtained (1.5 g, 47 %). *An*
32 *attempt to recrystallize the product in EtOH only led to partial oxidation of the phosphine.* ^1H

1 NMR (300 MHz, CDCl₃, δ /ppm) 7.48–7.41 (m, 2H), 7.39–7.26 (m, 12H), 5.80 (s, 1H), 4.15–
2 4.00 (m, 4H); ¹³C{¹H} NMR (100 MHz, CDCl₃, δ /ppm) 138.7 (d, J_{P-C} = 11.5 Hz), 138.5,
3 137.1 (d, J_{P-C} = 10.7 Hz), 133.9 (d, J_{P-C} = 19.5 Hz), 128.9, 128.7 (d, J_{P-C} = 7.0 Hz), 126.7 (d,
4 J_{P-C} = 7.0 Hz), 103.6, 65.5; ³¹P{¹H}-NMR (162 MHz, CDCl₃, δ /ppm) -5.6; HR-MS (ESI-
5 QTOF, pos) m/z calcd for C₂₁H₂₀O₂P: 335.1195 [M+H]⁺, found: 335.1201.

6 **2.2.3 4-(Diphenylphosphino)benzaldehyde P**. [57-59] 2-(Diphenylphosphino)-1,3-
7 dioxolane (1.5 g, 4.5 mmol) was dissolved in a toluene (10 mL) / water (1 mL) mixture
8 before addition of p-toluenesulfonic acid (20 mg, 0.1 mmol). The mixture was refluxed and
9 the reaction monitored by TLC. After completion, the mixture was let cool down to RT and
10 more water (5 mL) was added. The mixture was extracted 3 times with ethyl acetate. The
11 combined organic phases were washed 3 times with saturated Na₂CO₃, dried over Na₂SO₄,
12 filtered and concentrated to give a yellow oil. The crude was purified over silica gel
13 chromatography with CH₂Cl₂ as eluent to obtain P as a white solid (1.05 g, 81 %). ¹H-NMR
14 (300 MHz, CDCl₃, δ /ppm) 10.0 (s, 1H), 7.85–7.77 (m, 2H), 7.46–7.29 (m, 12H); ¹³C{¹H}-
15 NMR (100 MHz, CDCl₃, δ /ppm) 192.1, 146.6 (d, J_{P-C} = 15.6 Hz), 136.1, 135.9 (d, J_{P-C} = 10.5
16 Hz), 134.2 (d, J_{P-C} = 20.2 Hz), 133.7 (d, J_{P-C} = 18.5 Hz), 129.5, 128.9 (d, J_{P-C} = 7.4 Hz);
17 ³¹P{¹H}-NMR (162 MHz, CDCl₃, δ /ppm) -4.3; HR-MS (ESI-QTOF, pos) m/z calcd for
18 C₁₉H₁₆OP: 291.0933 [M+H]⁺, found: 291.0926.

19 **2.2.4 Synthesis of compounds P1-P4**. In a 10 mL microwave tube, P (200 mg, 0.69
20 mmol) and the corresponding acceptor group (0.65 mmol) were suspended in absolute
21 ethanol (4 mL). One drop of piperidine was added before sealing of the microwave tube. The
22 reaction was heated to 100 °C by microwave irradiation during 30 minutes. After cooling
23 down to RT, the precipitated dye was filtered and washed with cold ethanol. The dyes were
24 purified by column chromatography over silica gel using the eluent indicated.

25 **2.2.5 P1**. From P and 1 (130 mg). Eluent: CH₂Cl₂. Red solid (200 mg, 65 %). ¹H-
26 NMR (400 MHz, CD₂Cl₂, δ /ppm) 7.66–7.59 (m, 3H), 7.42–7.32 (m, 11H), 7.08 (d, J = 16.5
27 Hz, 2H), 1.78 (s, 6H); ¹³C{¹H}-NMR (125 MHz, CD₂Cl₂, δ /ppm) 175.8, 174.3, 147.0, 145.0
28 (d, J_{P-C} = 15.4 Hz), 136.5 (d, J_{P-C} = 11.1 Hz, 2C), 134.4 (d, J_{P-C} = 20.2 Hz), 134.3 (d, J_{P-C} =
29 18.3 Hz), 129.7 (2C), 129.2 (d, J_{P-C} = 7.3 Hz), 129.0 (d, J_{P-C} = 6.2 Hz), 115.9, 112.1, 111.5,
30 110.6, 100.8, 98.4, 26.6; ³¹P{¹H}-NMR (202 MHz, CD₂Cl₂, δ /ppm) -4.12; HR-MS (ESI-
31 QTOF, pos) m/z calcd for C₃₀H₂₃N₃OP: 472.1573 [M+H]⁺, found: 472.1558.

1 **2.2.6 P2.** From **P** and **2** (173 mg). Eluent: CH₂Cl₂/petroleum ether (v/v 1:1) to
2 CH₂Cl₂. Yellow solid (250 mg, 71 %). ¹H NMR (400 MHz, CD₂Cl₂, δ/ppm) 8.32 (d, *J* =
3 16.9 Hz, 1H), 8.08–8.03 (m, 2H), 7.70–7.62 (m, 3H), 7.59–7.54 (m, 2H), 7.41–7.33 (m,
4 12H), 7.26 (d, *J* = 16.9 Hz, 1H), 1.70 (s, 6H); ¹³C{¹H}-NMR (125 MHz, CD₂Cl₂, δ/ppm)
5 171.1, 165.0, 144.4, 142.9 (d, *J*_{P-C} = 14.3 Hz), 140.2, 136.9 (d, *J*_{P-C} = 11.3 Hz), 135.5, 134.6,
6 134.4 (d, *J*_{P-C} = 18.7 Hz), 134.3 (d, *J*_{P-C} = 20.1 Hz), 129.6, 129.5, 129.1 (d, *J*_{P-C} = 7.2 Hz),
7 128.9, 128.7 (d, *J*_{P-C} = 6.4 Hz), 124.4, 116.8, 85.7, 27.4; ³¹P{¹H}-NMR (202 MHz, CD₂Cl₂,
8 δ/ppm) -4.86; HR-MS (ESI-QTOF, pos) *m/z* calcd for C₃₂H₂₈O₄PS: 539.1440 [M+H]⁺,
9 found: 539.1425.

10 **2.2.7 P3.** From **P** and **3** (100 mg, 0.66 mmol.). Eluent: CH₂Cl₂. Red solid (140 mg,
11 51 %). ¹H NMR (400 MHz, CD₂Cl₂, δ/ppm) 7.68 (d, *J* = 16.5 Hz, 1H), 7.62–7.57 (m, 2H),
12 7.42–7.30 (m, 12H), 6.95 (d, *J* = 16.4 Hz, 1H), 1.67 (s, 6H); ¹³C{¹H}-NMR (125 MHz,
13 CD₂Cl₂, δ/ppm) 176.4, 166.3, 145.3, 143.4 (d, *J*_{P-C} = 14.9 Hz), 136.7 (d, *J*_{P-C} = 11.1 Hz),
14 134.7, 134.3 (d, *J*_{P-C} = 20.2 Hz), 134.3 (d, *J*_{P-C} = 18.8 Hz), 129.6, 129.1 (d, *J*_{P-C} = 7.2 Hz),
15 128.6 (d, *J*_{P-C} = 6.2 Hz), 116.0, 112.5, 99.6, 87.4, 26.1; ³¹P{¹H}-NMR (202 MHz, CD₂Cl₂,
16 δ/ppm) -4.67; HR-MS (ESI-QTOF, pos) *m/z* calcd for C₂₇H₂₃NO₂P: 424.1461 [M+H]⁺,
17 found: 424.1448.

18 **2.2.8 P4.** From **P** and **4** (121 mg). Eluent: CH₂Cl₂. Red solid (70 mg, 23 %). ¹H
19 NMR (400 MHz, CD₂Cl₂, δ/ppm) 7.51–7.47 (m, 2H), 7.40–7.28 (m, 12H), 7.07 (s, 2H), 6.85
20 (s, 1H), 2.61 (s, 2H), 1.48 (s, 2H), 1.07 (s, 6H); ¹³C{¹H}-NMR (125 MHz, CD₂Cl₂, δ/ppm)
21 169.7, 154.2, 140.2 (d, *J*_{P-C} = 13.3 Hz), 137.2 (d, *J*_{P-C} = 11.3 Hz), 136.6, 136.5, 134.32 (d, *J*_{P-}
22 *C* = 18.4 Hz), 134.2 (d, *J*_{P-C} = 19.8 Hz), 130.2, 129.4, 129.0 (d, *J*_{P-C} = 7.1 Hz), 127.8 (d, *J*_{P-C} =
23 6.6 Hz), 124.3, 113.9, 113.2, 79.3, 43.3, 39.5, 32.3, 28.1; ³¹P{¹H}-NMR (202 MHz, CD₂Cl₂,
24 δ/ppm)
25 -5.29; HR-MS (ESI-QTOF, pos) *m/z* calcd for C₃₁H₂₈N₂P: 459.1985 [M+H]⁺, found:
26 459.1975.

27 **2.3 Spectroscopy**

28 Absorption spectra were recorded on a JASCO V670 spectrophotometer. Excitation and
29 fluorescence emission spectra were recorded using a Horiba-Jobin Yvon Fluorolog-3
30 spectrofluorimeter equipped with a Hamamatsu R928 or water-cooled R2658 photomultiplier
31 tubes. Spectra were corrected for the intensity variations of both the excitation light source
32 (lamp and grating) and the emission spectral response (detector and grating). All solvents

1 were of spectrophotometric grade. Solid state measurements were performed using a
2 calibrated integrative sphere (model F-3018 from Horiba Jobin Yvon) collecting the full
3 emission (2π steradians covered with spectralon®), and quantum yields were measured as
4 described previously.[53]

5 Absorption and fluorescence spectra in acetone and in acetone/water mixtures were measured
6 for 10 μ M solutions. Suspensions were made directly in the quartz fluorescence cells. Water
7 and acetone were mixed in the cell in the proportion of the given water fraction (f_w) to give a
8 final volume of 2.5 mL. 25 μ L of stock dye solution (1 mM) in acetone were then quickly
9 injected into the solvent mixture. The mixture was then shaken several times by hand to
10 obtain the final suspension with a 10 μ M dye concentration. α values were calculated by
11 dividing the emission in acetone/water 10:90 mixture by the emission in acetone solution.
12 Solvatochromism was measured on 8 μ M (**P1**) and 4 μ M (**P2-P4**) solutions of the dyes in
13 toluene, CH₂Cl₂ or acetone.

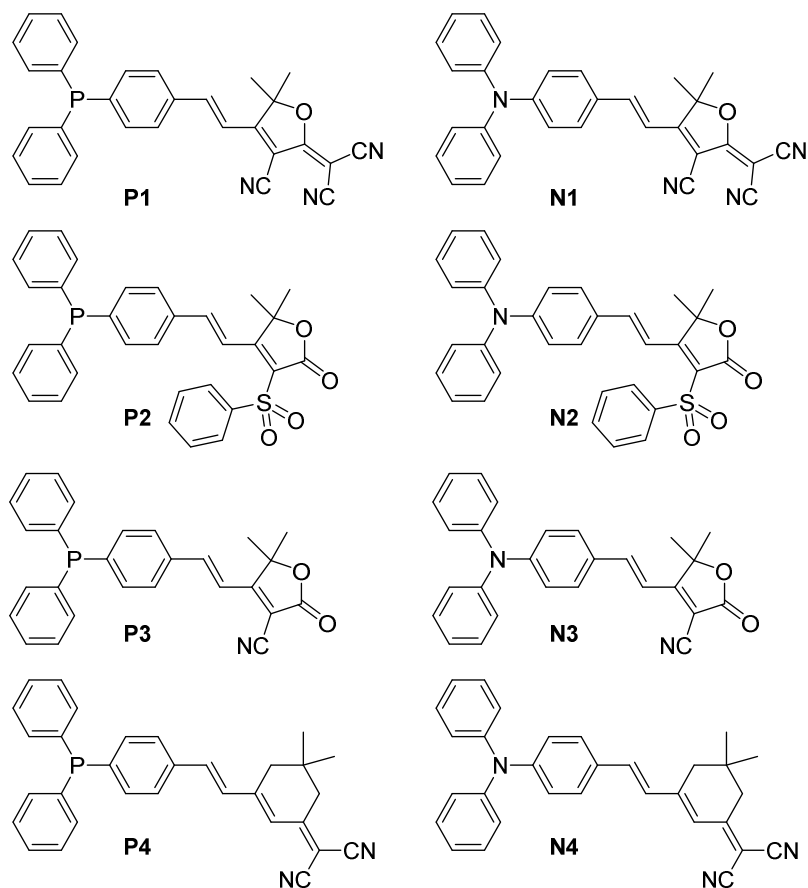
14 2.3.1 Crystallography

15 Single crystals of **P1** suitable for X-ray diffraction were grown by slow diffusion of a non-
16 solvent (EtOH) in a concentrated solution of dye (CHCl₃) at room temperature. CCDC
17 1563373 contains the supplementary crystallographic data for this paper. These data can be
18 obtained free of charge from The Cambridge Crystallographic Data Centre via
19 www.ccdc.cam.ac.uk/data_request/cif.

20 2.3.2 Computational details

21 All calculations were performed using Gaussian package.[60] At the ground state, the
22 structure of all the compounds was optimized at the DFT/6-31G(d) level of theory using the
23 M06-2X hybrid functional.[61] Bulk solvent effects (acetone) were considered using a
24 continuum solvation model (C-PCM).[62] For each compound, 10 vertical excitation energies
25 and the associated excited state densities of interest were computed at the TD-DFT level with
26 the same basis set and with the M06-2X functional. The charge transfers transitions were
27 characterized thanks to the $D_{C,T}$ index developed by Le Bahers *et al.* [63] using the cubegen
28 utility provided by the Gaussian package.

29 3 Results and discussion



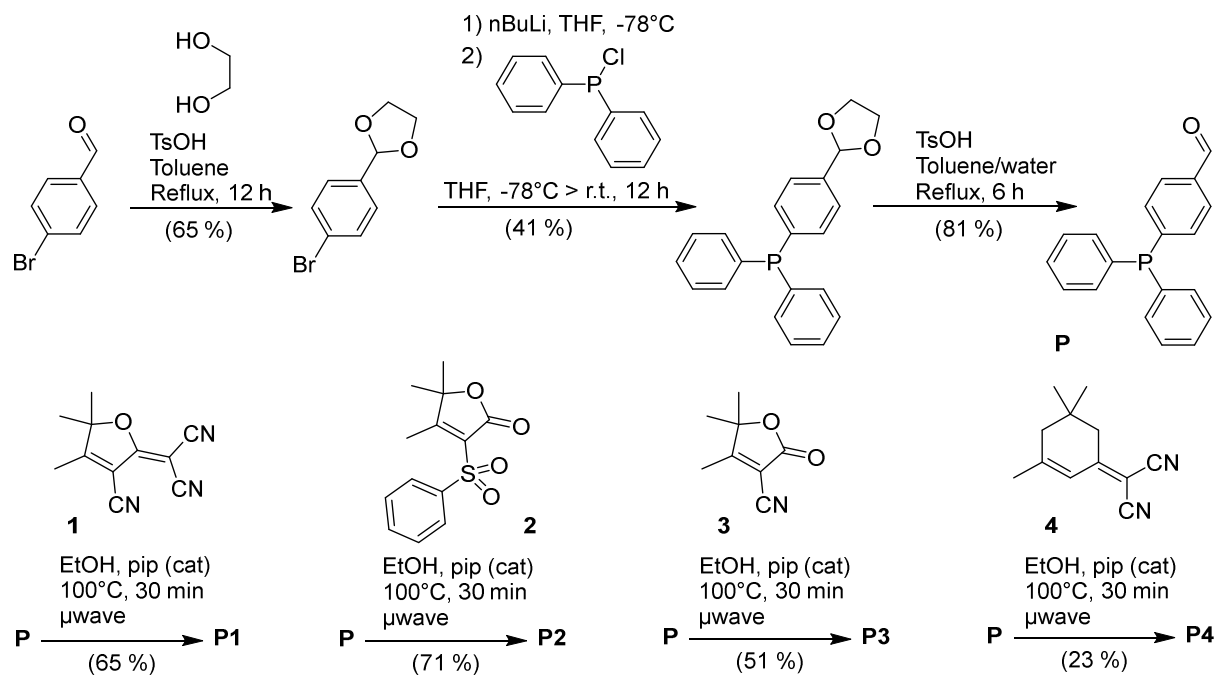
1

2 **Figure 1.** Structures of the P- λ 3 σ 3 chromophores **P1-P4** and nitrogen analogues **N1-N4**.

3 **3.1 Synthesis**

4 Synthesis of compounds **P1-P4** from 4-bromobenzaldehyde is depicted in Scheme 1. First,
 5 the aldehyde function was protected by formation of an acetal with ethylene glycol.[54-56]
 6 Then, the P-center was formed by a lithium-halogen exchange using *n*BuLi at -78°C followed
 7 by nucleophilic substitution on chlorodiphenylphosphine. Finally, deprotection in acidic
 8 conditions gave 4-(diphenylphosphino)benzaldehyde **P**.[57-59] Note that, in our hands, this
 9 four steps methodology offered a much better overall yield of 4-
 10 (diphenylphosphino)benzaldehyde (35 %) than direct palladium catalyzed phosphination of
 11 4-bromobenzaldehyde using triphenylphosphine.[64] Compounds **P1-P4** were obtained in
 12 moderate to good yield (23 %-71 %) by a Knoevenagel reaction with the active exocyclic
 13 methyl group of the corresponding electron-acceptors derivatives **1-4** [52] in ethanol using a
 14 catalytic amount of piperidine. The later step was performed under micro-wave irradiation,
 15 giving better yields than traditional heating.

1 The stability of the powder dyes to oxidation was verified by ^1H and ^{31}P NMR. After two
 2 years of storage at room temperature (15-30°C) under air, the NMR of the redissolved
 3 powder showed no P(V) peak in ^{31}P NMR, nor any change of the protons' chemical shift. On
 4 the other hand, colorless solutions of **P2** or **P3** in acetone turned slightly yellow after one
 5 week.

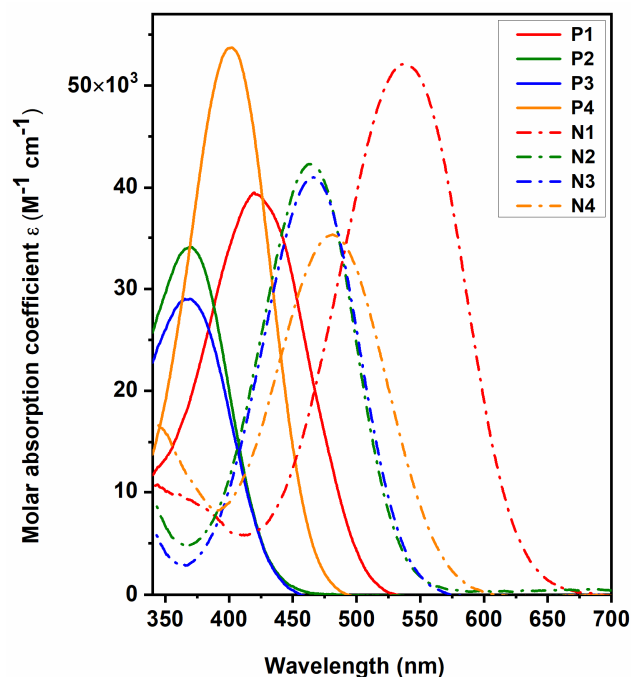


Scheme 1. Synthetic route to the target compounds **P1-P4**.

3.2 Spectroscopic properties in solution

9 The optical properties of the dyes were studied in dilute acetone solutions. Spectra are shown
 10 in Figure 2 and the optical properties are summarized in Table 1. The broad absorption of the
 11 dyes in the UV or visible range showed typical charge transfer transitions. For a given
 12 acceptor group, the absorption maxima were considerably blue-shifted for the P-dye
 13 compared to the amine dye. Whereas the absorption maxima of **N1-N4** were located between
 14 460 nm and 540 nm, the absorption maxima of **P1-P4** ranged between 370 nm and 420 nm,
 15 with only **P1** in the visible range. This blue-shift, of 5000 cm^{-1} on average, was likely due to
 16 the lower donating capacity of phosphorus compared to nitrogen caused by the tetrahedral
 17 geometry of the former.[14] As anticipated, for a given donor group, increasing the strength
 18 of the electron accepting part led to an increase in the charge transfer, visible by the red-shift
 19 of the absorption. Finally, molar absorption coefficients ϵ were in the range of 30 000 to
 20 50 000 $\text{M}^{-1}\text{cm}^{-1}$, which is very similar to what we previously reported for such small charge-
 21 transfer chromophores.[51, 52] Note that for both P- and N- compounds the donor group does

1 not seem to have a strong influence on the molar absorption coefficients values. A small
2 solvatochromism is observed in absorption for all the dyes (Figure SI 1 to SI 4, Table SI 1),
3 and is higher for P-dyes compared to N-dyes. The highest effect is observed for **P2** with a
4 1446 cm^{-1} difference between the maximum in acetone and in dichloromethane.



5
6 **Figure 2.** Absorption spectra of **P1-P4** (plain lines) and **N1-N4** (dotted lines) in dilute solution in acetone.

7 In a dilute solution at room temperature, N-based chromophores **N1-N4** showed a moderate
8 emission intensity that is strongly dependent on the solvent with a large red-shift, along with
9 decrease in the quantum yield emission when the solvent polarity is increased.[52] A
10 measurable emission was still obtained in polar acetone. On the contrary, P-based
11 chromophores **P1-P3** were not emissive in any solvent. Only **P4** showed a weak orange
12 fluorescence (centered at 600 nm) in toluene (Φ not measured, Figure SI 5).

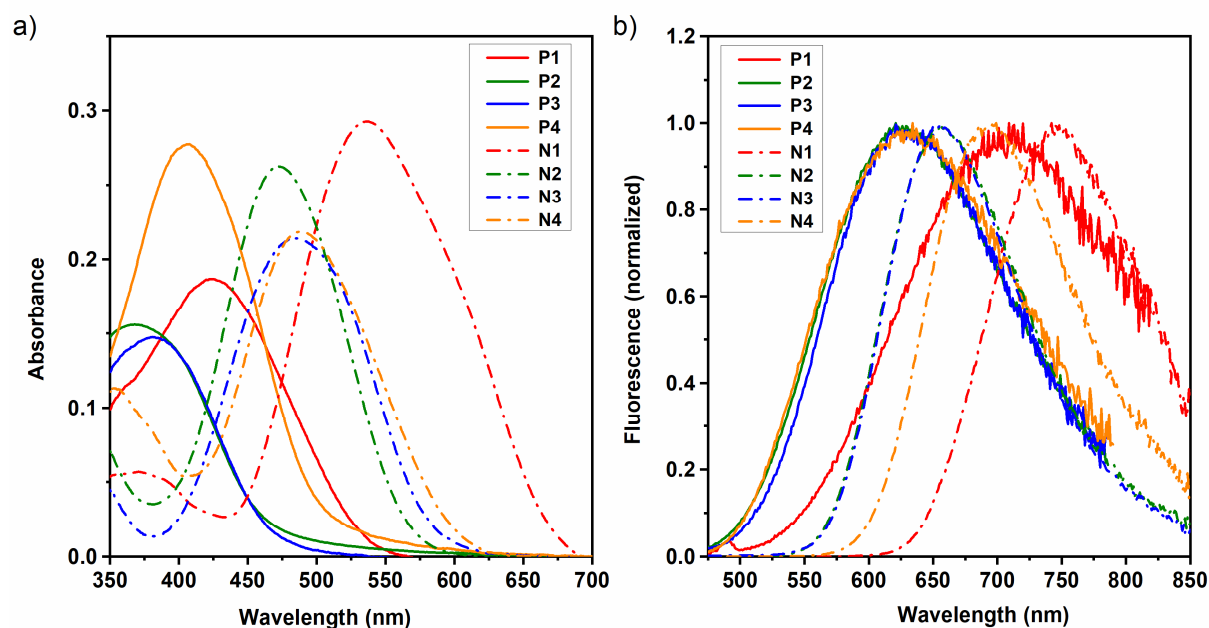
13 **3.3 Spectroscopic properties in the solid-state**

14 **3.3.1 Aggregation-induced emission (AIE) properties**

15 Interestingly, things considerably changed when studying the optical properties in the solid
16 state. We have previously shown that the N-chromophores exhibited aggregation induced
17 emission properties (AIE): the corresponding data are presented in Table 1.[51, 52] Nano-
18 precipitation experiments were therefore performed to access the eventual AIE properties of
19 the P-based chromophores. Absorption and emission spectra were recorded from different
20 acetone/water mixtures of **P2** ($10\text{ }\mu\text{M}$) with increased volume fractions of water (f_w). As

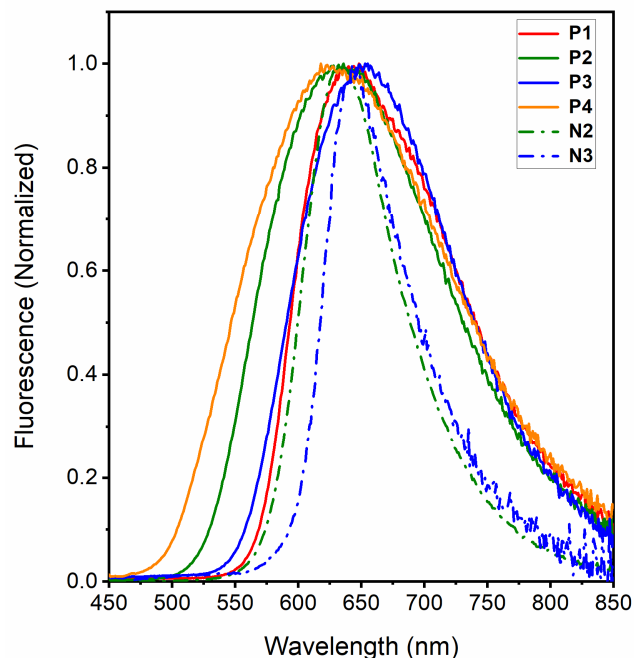
1 shown in Figure SI 6, increasing the water fraction of the acetone/water mixtures above a
2 critical water fraction ($f_w > 0.65$ here) resulted in the appearance of an orange fluorescence
3 ($\lambda_{em} = 630$ nm) as well as a severe broadening of the absorption spectra, which is
4 characteristic of AIE effect. A 170-fold increase of α_{AIE} (defined as the ratio in the
5 fluorescence intensity between the aggregate and the solution in pure acetone, $f_w = 0$) was
6 attained for $f_w = 0.9$. This is 17-fold more than for **N2** in the same conditions.

7 The other P-based chromophores **P1**, **P3** and **P4** also showed similar AIE properties in the
8 orange to far-red region, and only the data for an acetone/water ratio $f_w = 0.9$ are given in
9 Table 1 and Figure 3. The α_{AIE} observed for the P-dyes are 7- to 70-folds higher than for the
10 corresponding N-dyes. As observed for the dilute solution, the absorption spectra of the P-
11 chromophores aggregates were strongly blue-shifted compared to their N analogues (around
12 5000 cm^{-1}). Hypochromic shifts were also observed in emission, albeit much less pronounced
13 (around 1000 cm^{-1}). Indeed, the emission maxima obtained for the P-dyes ranged from 635 to
14 705 nm (against 655-750 nm for the N-dyes). Note the particularly long emission wavelength
15 for compound **P1** (705 nm), which is particularly interesting for the design of turn-on probe
16 for analytical or biological applications and is remarkable for a fluorophore with such a small
17 molecular weight. This is the consequence of a considerably larger Stokes shift for the four P-
18 based dye aggregates (9000 - 11000 cm^{-1}) than for their N-based analogues (5000 - 6000 cm^{-1}).
19 This can be attributed to consequent geometrical changes between the ground state and the
20 first excited state, as quantum chemical calculations revealed (*vide infra*).



21

1 **Figure 3.** a) Absorption and b) normalized emission spectra of dyes aggregates obtained in a 10:90
 2 acetone/water mixture (10 μ M)). The phosphorus based dyes **P1-P4** are represented using plain lines and the
 3 nitrogen based dyes **N1-N4** with dotted lines. $\lambda_{exc} = 410$ nm for P-dyes and $\lambda_{exc} = 490$ nm, for N-dyes except for
 4 **N1**, $\lambda_{exc} = 540$ nm.



5
 6 **Figure 4.** Crystal state fluorescence spectra of dyes **P1-P4** (plain lines) and **N2-N3** (dotted lines). $\lambda_{exc} = 390$ or
 7 400 nm for all dyes.

8 3.3.2 Emission in the crystalline state

9 As shown in Figure 4, P-based chromophores **P1-P4** are also emissive in crystalline powder.
 10 Emission maxima ranged from 620 nm (**P4**) to 650 nm (**P1**) for measured quantum yield of a
 11 few percent (Table 1). In comparison, only **N2** and **N3**, bearing the weaker acceptors, are
 12 emissive in crystalline powder, with quantum yields of 34 % at 635 nm and 8 % at 645 nm,
 13 respectively.[51, 52] Here again, the hypsochromic shift observed between P-based dyes and
 14 their N-analogues is small.

15 **Table 1.** Absorption maxima (λ_{max}^{abs}), molar absorptivity (ϵ), emission maximum (λ_{max}^{em}) for each dye in
 16 solution in acetone; Absorption and emission maxima (λ_{max}^{abs}), α_{AIE} and Stokes Shift ($\Delta\nu$) for nanoaggregates
 17 obtained in acetone/water mixture (10:90); Emission maximum (λ_{max}^{em}) and quantum yield (ϕ_F) in solid powder.

	Solution			Nanoaggregates				Solid	
	λ_{max}^{abs} (nm)	ϵ (L.mol ⁻¹ cm ⁻¹)	λ_{max}^{em} (nm)	λ_{max}^{abs} (nm)	λ_{max}^{em} (nm)	α_{AIE}^a	$\Delta\nu$ (cm ⁻¹)	λ_{max}^{em} (nm)	ϕ_F (%) ^b
P1	420	39 500	-	425	705	90	9 350	650	1
P2	365	34 100	-	370	630	170	11 150	635	5
P3	370	29 000	-	380	625	50	10 300	655	4
P4	400	53 700	-	405	635	35	8 950	620	7

N1	540	52 100	745	535	750	8	5 350	-	-
N2	465	42 300	670	470	665	10	6 250	635	34
N3	465	41 000	656	485	655	7	5 350	645	9
N4	480	35 300	689	490	700	0.5	6 100	-	-

^a Defined as the fluorescence intensity ratio between acetone/water mixture (10/90) and pure acetone solution;

^b Measured using a calibrated integrating sphere

3.4 Theoretical studies and comparison with crystal structures

To rationalize the optical properties observed, quantum chemical calculations were performed. A benchmark of exchange correlation functionals on the calculation of the S_0 - S_1 transition energies compared to experimental values identifies M062X as the best functional for our study (Table SI 2). This functional was used in the rest of the study.

3.4.1 Structural variations between the ground- and the first excited-state

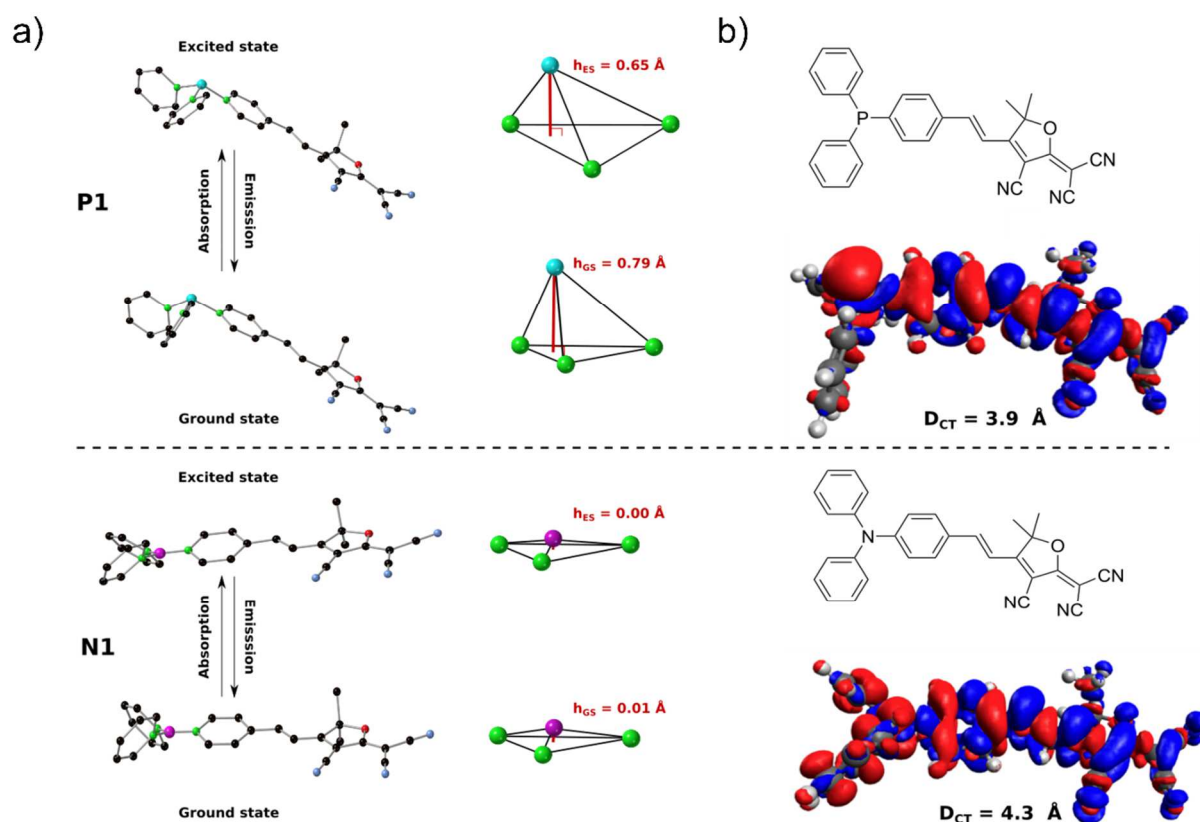
For the P-dyes **P1-P3**, considerable structural variations can be observed between the optimized structures of the ground state and first excited state in acetone, especially around the P-center. In the ground state, the P-centers adopt a trigonal pyramidal geometry, with an average height (h) of 0.79 Å for the pyramidal structure. Upon excitation, in the first excited state, the planarity of the compounds increases characterized by a decrease of the pyramid height of 0.20 Å on average. This increase of the planarity of the phosphorus donor and the conjugation of the π system is not observed for the **P4** compound which maintains the pyramidal geometry of its ground state (Table 2). Interestingly, this order of geometry reorganization according to the electron acceptor (0.00 for **P4**, 0.13 for **P1** and 0.22 for both **P2** and **P3**) perfectly matches with the order of Stokes shift values obtained experimentally (**P4** < **P1** < **P3** \approx **P2**) and the fact that **P4** is the only P-dye fluorescent in (apolar) solution.

By contrast, for the N-dyes **N1-N4**, the geometry around the N donor atom is trigonal planar, both in the ground states and in the first excited states, with an average height of 0.01 Å. The comparison between the ground states and excited states of **P1** and **N1** is given in Figure 5a.

3.4.2 Electronic density variations

The electronic density variations were also calculated and are represented in Figure 5b for **N1** and **P1** and in SI for the other dyes. The red (blue) area represents a decrease (respectively enhancement) of the electronic density during the transition. In both N-dyes and P-dyes, the electronic density of the donor is depleted and that of the acceptor is enriched, which is consistent with the character of the strong charge transfer. However, the depletion of the donor side is quite different depending on the donor atom. In the case of the $(C_6H_5)_2P$ - group,

1 the charge transfer mainly originates from the lone pair of the phosphorus atom, highly
 2 localized on the upper side of the chromophore plane as shown in Figure 5b. In the case of a
 3 $(C_6H_5)_2N$ - donor, there is a stronger contribution of the orbitals of the phenyls rings and the
 4 lone pair is localized on both sides of the chromophore plane. Quantitatively, we estimated
 5 the strength of the charge transfer associated to the force transition by computing the D_{CT}
 6 index (Table SI 4), a parameter defining the spatial extent associated to the transition as well
 7 as the associated fraction of electron transferred.[63] From P- to N-dyes, the average D_{CT}
 8 increases by around 10%, from 4 Å to 4.4 Å, consistent with the stronger charge transfer
 9 within the amine dyes, as well as the implication of the orbitals of the phenyls.



10
 11 **Figure 5** a) structural variations between the optimized structures of the ground state and the first excited state
 12 in acetone for **P1** (top) and **N1** (bottom) compounds. The optimized structures of both the ground and the
 13 excited states are shown on the left, while the pyramidal geometry around the P or N center is shown on the
 14 right. P and N-centers are represented in cyan and pink respectively, connected carbon atoms in green. b)
 15 Electronic density variations of **P1** (top) and **N1** (bottom) compounds. Red (blue) area represents a decrease
 16 (respectively enhancement) of the electronic density during the transition.

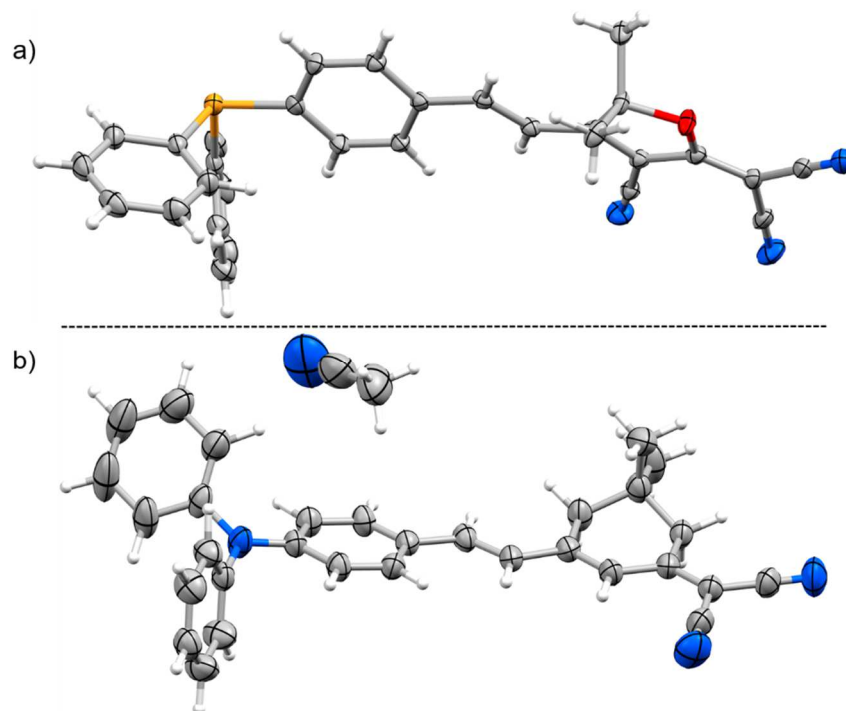
3.4.3 Comparison with X-ray crystal structures

To probe the phenomenon more deeply, we studied the crystalline structures. Crystals suitable for X-ray diffraction analysis were obtained for **P1**, by slow diffusion of ethanol in chloroform. We previously reported the crystal structures of N-dyes **N2**,^[51] **N3** ^[52] and **N4** ^[50]. Unfortunately, all attempts to obtain crystals for **N1** and other P-dyes **P2-P4** only produced thin needles, unsuitable for X-ray diffraction. So, despite the acceptor difference, we chose to compare the solid-state structures of **P1** and **N4**, selected as a model of N-dyes (Figure 6). The **N4** π system is quasi-planar, with only a small 10° angle between the acceptor and donor mean planes. In agreement with the calculations, the triphenylamino moiety adopts a trigonal planar configuration, with a pyramid height of 0.06 Å (Figure 6b, Fig SI 14). Note that **N2** and **N3** show very similar planarity in their crystal structures (Figure SI-11 to SI-13). The **P1** π system is very similar to that of **N4**, with a small 12° angle between the acceptor and donor mean planes. On the other hand, Figure 6 clearly shows the pyramidal configuration of phosphorus in **P1**. The measured pyramid height is 0.82 Å (Figure 6a, Figure SI-15), very close to the calculated value (0.79 Å) obtained by optimization of the ground state structure in acetone. Those geometry differences have consequences for the position of the lone pair, perpendicular to the π system for N-dyes and tilted to the back and to the side for P-dyes, thus, on the conjugation of the donor with the rest of the chromophore. All computationally obtained pyramid heights are given in Table 2, along with available DRX data. Finally, for both chromophores, neighbors are arranged in a dimeric head-to-tail configuration with an intermolecular distance of 3.2 Å for **N4** and 3.1 Å for **P1** (Figure SI 16). Despite the enhanced steric hindrance of the out-of-plane phenyls of **P1** compared to **N4**, neighboring dyes are actually closer in the crystal arrangement of compound **P1**. On a larger scale, the herringbone arrangement of **P1** dyes, as viewed down the crystallographic *a* axis (Figure SI 17), is usually considered as beneficial for solid state fluorescence.

Table 2. Heights for the pyramidal structure of the different compounds from DRX experiments (h^{RX}) or optimized structures of both ground and excited states from DFT/M062X calculations (respectively h^{DFT}_{GS} and h^{DFT}_{ES}).

	h^{RX}_{GS} (Å)	h^{DFT}_{GS} (Å)	h^{DFT}_{ES} (Å)
N1	--	0.01	0.00
N2	0.07	0.01	0.00
N3	0.05	0.02	0.01
N4	0.06	0.01	0.01
P1	0.82	0.79	0.66

P2	--	0.79	0.57
P3	--	0.80	0.57
P4	--	0.79	0.78



1
2 **Figure 6.** Comparative views of the X-ray crystal structures of a) **P1** and b) **N4**, showing the pyramidal
3 configuration of the phosphorus and the trigonal planar configuration of the nitrogen atom (ORTEP views with
4 50% probability displacement ellipsoids. H atoms are omitted for clarity. Compound **N4** crystallized with an
5 acetonitrile molecule).

6 **4 Conclusion**

7 The synthesis of four novel dyes based on the diphenylphosphino donor-group enabled us to
8 study their optical properties in solution and in the solid state and compare them with the
9 diphenylamino-analogues. Despite being quenched in solution, probably due to the
10 intramolecular planarization movement of the phosphine donor, they light up in solid state
11 (amorphous aggregates or crystalline powder) as typical AIE was demonstrated by
12 nanoprecipitation procedure involving a solvent shifting process. Phosphine aggregates
13 showed higher fluorescence turn-on coefficients upon aggregation (170-fold increase
14 emission for **P2**) than their amine analogues, but above all much larger Stokes shift (10 000
15 cm^{-1} on average), that can be attributed to large conformational changes around the P-atom
16 between the ground state and the first excited state. In fine, we believe that the
17 diphenylphosphino- can be an interesting donor group for the design of large Stoke shift
18 fluorophores and could be used to control intramolecular packing in the solid-state, or could

1 even be used in molecular machines as they are capable of producing small but reproducible
2 planarity change upon light absorption.

3 **References**

- 4 [1] Li D, Zhang H, Wang Y. Four-Coordinate Organoboron Compounds for Organic Light-
5 Emitting Diodes (OLEDs). *Chem Soc Rev* 2013;42(21):8416-33.
6 <https://doi.org/10.1039/c3cs60170f>.
- 7 [2] Mellerup SK, Wang S. Boron-Based Stimuli Responsive Materials. *Chem Soc Rev*
8 2019;48(13):3537-49. <https://doi.org/10.1039/c9cs00153k>.
- 9 [3] Hirai M, Tanaka N, Sakai M, Yamaguchi S. Structurally Constrained Boron-, Nitrogen-,
10 Silicon-, and Phosphorus-Centered Polycyclic π -Conjugated Systems. *Chem Rev*
11 2019;119(14):8291-331. <https://doi.org/10.1021/acs.chemrev.8b00637>.
- 12 [4] Zhao Q, Wang J, Freeman JL, Murphy-Jolly M, Wright AM, Scardino DJ, Hammer NI,
13 Lawson CM, Gray GM. Syntheses, and Optical, Fluorescence, and Nonlinear Optical
14 Characterization of Phosphine-Substituted Terthiophenes. *Inorg Chem* 2011;50(5):2015-27.
15 <https://doi.org/10.1021/ic101624y>.
- 16 [5] Zhao Q, Freeman JL, Wang J, Zhang Y, Hamilton TP, Lawson CM, Gray GM. Syntheses,
17 X-ray Crystal Structures, and Optical, Fluorescence, and Nonlinear Optical Characterizations
18 of Diphenylphosphino-Substituted Bithiophenes. *Inorg Chem* 2012;51(4):2016-30.
19 <https://doi.org/10.1021/ic201309k>.
- 20 [6] Freeman JL, Zhao Q, Zhang Y, Wang J, Lawson CM, Gray GM. Synthesis, Linear and
21 Nonlinear Optical Properties of Phosphonato-Substituted Bithiophenes Derived from 2,2'-
22 Biphenol. *Dalton Trans* 2013;42(39):14281-97. <https://doi.org/10.1039/c3dt51499d>.
- 23 [7] Allen DW, Mifflin JP, Skabara PJ. Synthesis and Solvatochromism of Some Dipolar
24 Aryl-phosphonium and -Phosphine Oxide Systems. *J Organomet Chem* 2000;601(2):293-8.
25 [https://doi.org/10.1016/S0022-328X\(00\)00085-1](https://doi.org/10.1016/S0022-328X(00)00085-1).
- 26 [8] Lambert C, Gaschler W, Nöll G, Weber M, Schmäzlin E, Bräuchle C, Meerholz K.
27 Cationic π -Electron Systems with High Quadratic Hyperpolarisability. *J Chem Soc, Perkin*
28 *Trans 2* 2001;(6):964-74. <https://doi.org/10.1039/b009664b>.
- 29 [9] Belyaev A, Cheng Y-H, Liu Z-Y, Karttunen AJ, Chou P-T, Koshevoy IO. A Facile
30 Molecular Machine: Optically Triggered Counterion Migration by Charge Transfer of Linear
31 Donor- π -Acceptor Phosphonium Fluorophores. *Angew Chem Int Ed* 2019;58(38):13456-65.
32 <https://doi.org/10.1002/anie.201906929>.

- 1 [10] Alain-Rizzo V, Drouin-Kucma D, Rouxel C, Samb I, Bell J, Toullec PY, Michelet V,
2 Leray I, Blanchard-Desce M. Synthesis, Photophysical, and Two-Photon Absorption
3 Properties of Elongated Phosphane Oxide and Sulfide Derivatives. *Chem Asian J*
4 2011;6(4):1080-91. <https://doi.org/10.1002/asia.201000681>.
- 5 [11] Bell J, Samb I, Toullec PY, Michelet V, Leray I. Synthesis and Complexing Properties
6 of Molecular Probes Linked with Fluorescent Phosphane Oxide Derivatives. *J Photochem*
7 *Photobiol A* 2016;318:25-32. <https://doi.org/10.1016/j.jphotochem.2015.11.017>.
- 8 [12] Ha-Thi M-H, Souchon V, Hamdi A, Métivier R, Alain V, Nakatani K, Lacroix PG,
9 Genêt J-P, Michelet V, Leray I. Synthesis of Novel Rod-Shaped and Star-Shaped Fluorescent
10 Phosphane Oxides—Nonlinear Optical Properties and Photophysical Properties. *Chem Eur J*
11 2006;12(35):9056-65. <https://doi.org/10.1002/chem.200600464>.
- 12 [13] Lambert C, Schmäzlin E, Meerholz K, Bräuchle C. Synthesis and Nonlinear Optical
13 Properties of Three-Dimensional Phosphonium Ion Chromophores. *Chem Eur J*
14 1998;4(3):512-21. [https://doi.org/10.1002/\(sici\)1521-3765\(19980310\)4:3<512::aid-
15 chem512>3.0.co;2-7](https://doi.org/10.1002/(sici)1521-3765(19980310)4:3<512::aid-chem512>3.0.co;2-7).
- 16 [14] Baumgartner T, Réau R. Organophosphorus π -Conjugated Materials. *Chem Rev*
17 2006;106(11):4681-727. <https://doi.org/10.1021/cr040179m>.
- 18 [15] Crassous J, Réau R. π -Conjugated Phosphole Derivatives: Synthesis, Optoelectronic
19 Functions and Coordination Chemistry. *Dalton Trans* 2008;(48):6865-76.
20 <https://doi.org/10.1039/b810976a>.
- 21 [16] Bouit P-A, Escande A, Szűcs R, Szieberth D, Lescop C, Nyulászi L, Hissler M, Réau R.
22 Dibenzophosphapentaphenes: Exploiting P Chemistry for Gap Fine-Tuning and
23 Coordination-Driven Assembly of Planar Polycyclic Aromatic Hydrocarbons. *J Am Chem*
24 *Soc* 2012;134(15):6524-7. <https://doi.org/10.1021/ja300171y>.
- 25 [17] Stolar M, Baumgartner T. Phosphorus-Containing Materials for Organic Electronics.
26 *Chem Asian J* 2014;9(5):1212-25. <https://doi.org/10.1002/asia.201301670>.
- 27 [18] Baumgartner T. Insights on the Design and Electron-Acceptor Properties of Conjugated
28 Organophosphorus Materials. *Acc Chem Res* 2014;47(5):1613-22.
29 <https://doi.org/10.1021/ar500084b>.
- 30 [19] Duffy MP, Delaunay W, Bouit PA, Hissler M. π -Conjugated Phospholes and Their
31 Incorporation into Devices: Components with a Great Deal of Potential. *Chem Soc Rev*
32 2016;45(19):5296-310. <https://doi.org/10.1039/c6cs00257a>.

- 1 [20] Zhou Y, Yang S, Li J, He G, Duan Z, Mathey F. Phosphorus and Silicon-Bridged
2 Stilbenes: Synthesis and Optoelectronic Properties. *Dalton Trans* 2016;45(45):18308-12.
3 <https://doi.org/10.1039/c6dt03489f>.
- 4 [21] Shameem MA, Orthaber A. Organophosphorus Compounds in Organic Electronics.
5 *Chem Eur J* 2016;22(31):10718-35. <https://doi.org/10.1002/chem.201600005>.
- 6 [22] Wang C, Fukazawa A, Tanabe Y, Inai N, Yokogawa D, Yamaguchi S. Water-Soluble
7 Phospholo[3,2-b]phosphole-P,P'-Dioxide-Based Fluorescent Dyes with High Photostability.
8 *Chem Asian J* 2018;13(12):1616-24. <https://doi.org/10.1002/asia.201800533>.
- 9 [23] Higashino T, Ishida K, Satoh T, Matano Y, Imahori H. Phosphole–Thiophene Hybrid: A
10 Dual Role of Dithieno[3,4-b:3',4'-d]phosphole as Electron Acceptor and Electron Donor. *J*
11 *Org Chem* 2018;83(6):3397-402. <https://doi.org/10.1021/acs.joc.8b00030>.
- 12 [24] Fukazawa A, Yamada H, Yamaguchi S. Phosphonium- and Borate-Bridged Zwitterionic
13 Ladder Stilbene and Its Extended Analogues. *Angew Chem Int Ed* 2008;47(30):5582-5.
14 <https://doi.org/10.1002/anie.200801834>.
- 15 [25] Chai X, Cui X, Wang B, Yang F, Cai Y, Wu Q, Wang T. Near-Infrared Phosphorus-
16 Substituted Rhodamine with Emission Wavelength above 700 nm for Bioimaging. *Chem Eur*
17 *J* 2015;21(47):16754-8. <https://doi.org/10.1002/chem.201502921>.
- 18 [26] Jiang X-D, Zhao J, Xi D, Yu H, Guan J, Li S, Sun C-L, Xiao L-J. A New Water-Soluble
19 Phosphorus-Dipyrromethene and Phosphorus-Azadipyrromethene Dye: PODIPY/aza-
20 PODIPY. *Chem Eur J* 2015;21(16):6079-82. <https://doi.org/10.1002/chem.201406535>.
- 21 [27] Zhou X, Lai R, Beck JR, Li H, Stains CI. Nebraska Red: a Phosphinate-Based Near-
22 Infrared Fluorophore Scaffold for Chemical Biology Applications. *Chem Commun*
23 2016;52(83):12290-3. <https://doi.org/10.1039/c6cc05717a>.
- 24 [28] Fukazawa A, Suda S, Taki M, Yamaguchi E, Grzybowski M, Sato Y, Higashiyama T,
25 Yamaguchi S. Phospha-Fluorescein: a Red-Emissive Fluorescein Analogue with High
26 Photobleaching Resistance. *Chem Commun* 2016;52(6):1120-3.
27 <https://doi.org/10.1039/c5cc09345g>.
- 28 [29] Fukazawa A, Usuba J, Adler RA, Yamaguchi S. Synthesis of Seminaphtho-Phospha-
29 Fluorescein Dyes Based on the Consecutive Arylation of Aryldichlorophosphines. *Chem*
30 *Commun* 2017;53(61):8565-8. <https://doi.org/10.1039/c7cc04323f>.
- 31 [30] Grzybowski M, Taki M, Yamaguchi S. Selective Conversion of P=O-Bridged
32 Rhodamines into P=O-Rhodols: Solvatochromic Near-Infrared Fluorophores. *Chem Eur J*
33 2017;23(53):13028-32. <https://doi.org/10.1002/chem.201703456>.

- 1 [31] Hashimoto N, Umamo R, Ochi Y, Shimahara K, Nakamura J, Mori S, Ohta H, Watanabe
2 Y, Hayashi M. Synthesis and Photophysical Properties of λ^5 -Phosphinines as a Tunable
3 Fluorophore. *J Am Chem Soc* 2018;140(6):2046-9. <https://doi.org/10.1021/jacs.7b13018>.
- 4 [32] Grzybowski M, Taki M, Senda K, Sato Y, Ariyoshi T, Okada Y, Kawakami R, Imamura
5 T, Yamaguchi S. A Highly Photostable Near-Infrared Labeling Agent Based on a Phospha-
6 rhodamine for Long-Term and Deep Imaging. *Angew Chem Int Ed* 2018;57(32):10137-41.
7 <https://doi.org/10.1002/anie.201804731>.
- 8 [33] Ogasawara H, Grzybowski M, Hosokawa R, Sato Y, Taki M, Yamaguchi S. A Far-Red
9 Fluorescent Probe Based on a Phospha-Fluorescein Scaffold for Cytosolic Calcium Imaging.
10 *Chem Commun* 2018;54(3):299-302. <https://doi.org/10.1039/c7cc07344e>.
- 11 [34] Wang L, Du W, Hu Z, Uvdal K, Li L, Huang W. Hybrid Rhodamine Fluorophores in the
12 Visible/NIR Region for Biological Imaging. *Angew Chem Int Ed* 2019;58(40):14026-43.
13 <https://doi.org/10.1002/anie.201901061>.
- 14 [35] Belyaev A, Chen Y-T, Liu Z-Y, Hindenberg P, Wu C-H, Chou P-T, Romero-Nieto C,
15 Koshevoy IO. Intramolecular Phosphacyclization: Polyaromatic Phosphonium P-
16 Heterocycles with Wide-Tuning Optical Properties. *Chem Eur J* 2019;25(25):6332-41.
17 <https://doi.org/10.1002/chem.201900136>.
- 18 [36] Bard JP, Bates HJ, Deng C-L, Zakharov LN, Johnson DW, Haley MM. Amplification of
19 the Quantum Yields of 2- λ^5 -Phosphaquinolin-2-ones through Phosphorus Center
20 Modification. *J Org Chem* 2020;85(1):85-91. <https://doi.org/10.1021/acs.joc.9b02132>.
- 21 [37] Sauer M, Nasufovic V, Arndt H-D, Vilotijevic I. Robust Synthesis of NIR-Emissive P-
22 Rhodamine Fluorophores. *Org Biomol Chem* 2020;18(8):1567-71.
23 <https://doi.org/10.1039/d0ob00189a>.
- 24 [38] Davies LH, Harrington RW, Clegg W, Higham LJ. $^B\text{R}_2\text{BodPR}_2$: Highly Fluorescent
25 Alternatives to PPh_3 and PhPCy_2 . *Dalton Trans* 2014;43(36):13485-99.
26 <https://doi.org/10.1039/c4dt00704b>.
- 27 [39] Davies LH, Stewart B, Harrington RW, Clegg W, Higham LJ. Air-Stable, Highly
28 Fluorescent Primary Phosphanes. *Angew Chem Int Ed* 2012;51(20):4921-4.
29 <https://doi.org/10.1002/anie.201108416>.
- 30 [40] Onoda M, Tokuyama H, Uchiyama S, Mawatari K-i, Santa T, Kaneko K, Imai K,
31 Nakagomi K. Fluorescence Enhancement by Hydroperoxides Based on a Change in the
32 Intramolecular Charge Transfer Character of Benzofurazan. *Chem Commun* 2005;(14):1848-
33 50. <https://doi.org/10.1039/b500419e>.

- 1 [41] Tirla A, Rivera-Fuentes P. Development of a Photoactivatable Phosphine Probe for
2 Induction of Intracellular Reductive Stress with Single-Cell Precision. *Angew Chem Int Ed*
3 2016;55(47):14709-12. <https://doi.org/10.1002/anie.201608779>.
- 4 [42] Hatakeyama T, Hashimoto S, Nakamura M. Tandem Phospha-Friedel–Crafts Reaction
5 toward Curved π -Conjugated Frameworks with a Phosphorus Ring Junction. *Org Lett*
6 2011;13(8):2130-3. <https://doi.org/10.1021/ol200571s>.
- 7 [43] Smith JN, Hook JM, Lucas NT. Superphenylphosphines: Nanographene-Based Ligands
8 That Control Coordination Geometry and Drive Supramolecular Assembly. *J Am Chem Soc*
9 2018;140(3):1131-41. <https://doi.org/10.1021/jacs.7b12251>.
- 10 [44] Madrigal LG, Spangler CW. The Synthesis of Diphenylpolyenes and PPV-Oligomers
11 Incorporating Diphenylphosphino Donor Groups. *MRS Proceedings*. 1999;561:75.
12 <https://doi.org/10.1557/PROC-561-75>.
- 13 [45] Madrigal L, Kuhl K, Spangler C. Photonic Properties of Dendrons and Dendrimers
14 Incorporating Bis-(Diphenylphosphino)Diphenylpolyenes. *MRS Proceedings*.
15 2011;598:BB8.9. <https://doi.org/10.1557/PROC-598-BB8.9>.
- 16 [46] Madrigal L, Spangler C. Diphenylphosphino-Substituted Diphenylpolyenes for
17 Applications in Nonlinear Optics. *Proc SPIE*. 1999;3796. <https://doi.org/10.1117/12.368275>.
- 18 [47] Yuan Z, Taylor NJ, Marder TB, Williams ID, Kurtz SK, Cheng L-T. Three Coordinate
19 Phosphorus and Boron as π -Donor and π -Acceptor Moieties Respectively, in Conjugated
20 Organic Molecules for Nonlinear Optics: Crystal and Molecular Structures of *E*-Ph–
21 CH=CH–B(mes)₂, *E*-4-MeO–C₆H₄–CH=CH–B(mes)₂, and *E*-Ph₂P–CH=CH–B(mes)₂ [mes =
22 2,4,6-Me₃C₆H₂]. *J Chem Soc, Chem Commun* 1990;(21):1489-92.
23 <https://doi.org/10.1039/c39900001489>.
- 24 [48] Agou T, Kobayashi J, Kawashima T. Dibenzophosphaborin: A Hetero- π -conjugated
25 Molecule with Fluorescent Properties Based on Intramolecular Charge Transfer between
26 Phosphorus and Boron Atoms. *Org Lett* 2005;7(20):4373-6.
27 <https://doi.org/10.1021/ol051537q>.
- 28 [49] He X, Borau-Garcia J, Woo AYY, Trudel S, Baumgartner T. Dithieno[3,2-*c*:2',3'-*e*]-2,7-
29 diketophosphepin: A Unique Building Block for Multifunctional π -Conjugated Materials. *J*
30 *Am Chem Soc* 2013;135(3):1137-47. <https://doi.org/10.1021/ja310680x>.
- 31 [50] Massin J, Dayoub W, Mulatier J-C, Aronica C, Bretonnière Y, Andraud C. Near-
32 Infrared Solid-State Emitters Based on Isophorone: Synthesis, Crystal Structure and

1 Spectroscopic Properties. *Chem Mater* 2011;23(3):862-73.
2 <https://doi.org/10.1021/cm102165r>.

3 [51] Yan X, Remond M, Zheng Z, Hoibian E, Soulage C, Chambert S, Andraud C, Van der
4 Sanden B, Ganachaud F, Bretonnière Y, Bernard J. General and Scalable Approach to Bright,
5 Stable, and Functional AIE Fluorogen Colloidal Nanocrystals for in Vivo Imaging. *ACS*
6 *Appl Mater Interfaces* 2018;10(30):25154-65. <https://doi.org/10.1021/acsami.8b07859>.

7 [52] Redon S, Eucat G, Ipuý M, Jeanneau E, Gautier-Luneau I, Ibanez A, Andraud C,
8 Bretonnière Y. Tuning the Solid-State Emission of Small Push-Pull Dipolar Dyes to the Far-
9 Red Through Variation of the Electron-Acceptor Group. *Dyes Pigm* 2018;156:116-32.
10 <https://doi.org/10.1016/j.dyepig.2018.03.049>.

11 [53] Ipuý M, Liao Y-Y, Jeanneau E, Baldeck PL, Bretonnière Y, Andraud C. Solid State Red
12 Biphonic Excited Emission from Small Dipolar Fluorophores. *J Mater Chem C*
13 2016;4(4):766-79. <https://doi.org/10.1039/c5tc03465e>.

14 [54] Nishi H, Namari T, Kobatake S. Photochromic polymers bearing various diarylethene
15 chromophores as the pendant: synthesis, optical properties, and multicolor photochromism. *J*
16 *Mater Chem* 2011;21(43):17249-58. <https://doi.org/10.1039/c1jm12707a>.

17 [55] Mei J, Wang J, Qin A, Zhao H, Yuan W, Zhao Z, Sung HHY, Deng C, Zhang S,
18 Williams ID, Sun JZ, Tang BZ. Construction of soft porous crystal with silole derivative:
19 strategy of framework design, multiple structural transformability and
20 mechanofluorochromism. *J Mater Chem* 2012;22(10):4290-8.
21 <https://doi.org/10.1039/c1jm12673c>.

22 [56] Xu G, Lei H, Zhou G, Zhang C, Xie L, Zhang W, Cao R. Boosting hydrogen evolution
23 by using covalent frameworks of fluorinated cobalt porphyrins supported on carbon
24 nanotubes. *Chem Commun* 2019;55(84):12647-50. <https://doi.org/10.1039/C9CC06916J>.

25 [57] Hon Y-S, Lee C-F, Chen R-J, Szu P-H. Acetonitriletriphenylphosphonium bromide and its
26 polymer-supported analogues as catalysts in protection and deprotection of alcohols as alkyl
27 vinyl ethers. *Tetrahedron* 2001;57(28):5991-6001.
28 [https://doi.org/https://doi.org/10.1016/S0040-4020\(01\)00558-0](https://doi.org/https://doi.org/10.1016/S0040-4020(01)00558-0).

29 [58] Xia X, Toy PH. Polyethyleneimine-Supported Triphenylphosphine and Its Use as a
30 Highly Loaded Bifunctional Polymeric Reagent in Chromatography-Free One-Pot Wittig
31 Reactions. *Synlett* 2015;26(12):1737-43. <https://doi.org/10.1055/s-0034-1380810>.

1 [59] García-Álvarez R, Díez J, Crochet P, Cadierno V. Arene–Ruthenium(II) Complexes
2 Containing Amino–Phosphine Ligands as Catalysts for Nitrile Hydration Reactions.
3 *Organometallics* 2010;29(17):3955-65. <https://doi.org/10.1021/om1006227>.

4 [60] Frisch MJ, Trucks GW, Schlegel HB, Scuseria GE, Robb MA, Cheeseman JR, Scalmani
5 G, Barone V, Petersson GA, Nakatsuji H, Li X, Caricato M, Marenich AV, Bloino J, Janesko
6 BG, Gomperts R, Mennucci B, Hratchian HP, Ortiz JV, Izmaylov AF, Sonnenberg JL,
7 Williams, Ding F, Lipparini F, Egidi F, Goings J, Peng B, Petrone A, Henderson T,
8 Ranasinghe D, Zakrzewski VG, Gao J, Rega N, Zheng G, Liang W, Hada M, Ehara M,
9 Toyota K, Fukuda R, Hasegawa J, Ishida M, Nakajima T, Honda Y, Kitao O, Nakai H,
10 Vreven T, Throssell K, Montgomery Jr. JA, Peralta JE, Ogliaro F, Bearpark MJ, Heyd JJ,
11 Brothers EN, Kudin KN, Staroverov VN, Keith TA, Kobayashi R, Normand J, Raghavachari
12 K, Rendell AP, Burant JC, Iyengar SS, Tomasi J, Cossi M, Millam JM, Klene M, Adamo C,
13 Cammi R, Ochterski JW, Martin RL, Morokuma K, Farkas O, Foresman JB, Fox DJ.
14 *Gaussian 16 Rev. C.01*. Wallingford, CT2016.

15 [61] Zhao Y, Truhlar DG. The M06 Suite of Density Functionals for Main Group
16 Thermochemistry, Thermochemical Kinetics, Noncovalent Interactions, Excited States, and
17 Transition Elements: Two New Functionals and Systematic Testing of Four M06-class
18 Functionals and 12 Other Functionals. *Theor Chem Acc* 2008;120(1):215-41.
19 <https://doi.org/10.1007/s00214-007-0310-x>.

20 [62] Cossi M, Rega N, Scalmani G, Barone V. Energies, Structures, and Electronic Properties
21 of Molecules in Solution with the C-PCM Solvation Model. *J Comput Chem* 2003;24(6):669-
22 81. <https://doi.org/10.1002/jcc.10189>.

23 [63] Le Bahers T, Adamo C, Ciofini I. A Qualitative Index of Spatial Extent in Charge-
24 Transfer Excitations. *J Chem Theory Comput* 2011;7(8):2498-506.
25 <https://doi.org/10.1021/ct200308m>.

26 [64] Kwong FY, Lai CW, Yu M, Chan KS. Application of Palladium-Catalyzed Pd–Aryl/P–
27 Aryl Exchanges: Preparation of Functionalized Aryl Phosphines by Phosphination of Aryl
28 Bromides Using Triarylphosphines. *Tetrahedron* 2004;60(26):5635-45.
29 <https://doi.org/10.1016/j.tet.2004.04.085>.

30